

The Enhancement of Photodegradation Efficiency Using Pt-TiO₂ Catalyst

F. B. Li^{1,2} and X. Z. Li^{1*}

¹*Department of Civil and Structural Engineering, The Hong Kong Polytechnic University, Hunghom, Kowloon, Hong Kong, Fax: (852) 2334 6389; Email: cexzli@polyu.edu.hk*

²*Guangdong Key Laboratory of Agro-Environment Integrated Control, Guangdong Institute of Eco-Environment and Soil Science, Leyiju, Guangzhou, 510650, P. R. China*

Abstract

This study investigates the mechanism of photosensitization and the recombination of excited electron-hole pairs affected by depositing platinum (Pt) on the surface of titanium dioxide (TiO₂). A new catalyst of Pt-TiO₂ was prepared by a photoreduction process. Being model reactions, the photocatalytic oxidation of methylene blue and methyl orange in aqueous solutions using the Pt-TiO₂ catalyst was carried out under either UV or visible light irradiation. The experimental results indicate that an optimal content of 0.75% Pt-TiO₂ achieves the best photocatalytic performance of methylene blue and methyl orange degradation and that the Pt-TiO₂ catalyst can be sensitized by visible light. The interaction of Pt and TiO₂ was investigated by means of UV-visible absorption spectra, photoluminescence emission spectra, and X-ray photoelectron emission spectroscopy. The Pt⁰, Pt²⁺ and Pt⁴⁺ species existing on the surface of Pt-TiO₂, and the Ti³⁺ species existing in its lattice may form a defect energy level. The Pt impurities,

* Author whom all correspondence should be addressed to

including Pt, Pt(OH)₂, and PtO₂, and the defect energy level absorb visible light more efficiently in comparison with the pure TiO₂ and hinder the recombination rate of excited electron/hole pairs.

Keywords: Titanium dioxide; Pt; Photoluminescence spectroscopy; Methylene blue; Methyl orange; Photosensitization

1. Introduction

The preferential use of titanium dioxide (TiO₂) in the photocatalytic degradation of organic pollutants is based on its high oxidative power, photostability, and nontoxicity (Hoffmann et al., 1995; Goswami, 1997). However, photocatalysis has not been widely applied to treat wastewater in industry, as its reaction rate is not high enough owing to a quick recombination of charge carriers (Linsebigler et al., 1995). Numerous investigations have reported that it is an effective method to add Group VIII metals to TiO₂-based photocatalytic systems to enhance the photocatalytic reaction rate (Serpone and Pelizzetti, 1989; Yang et al., 1997; Vorontsov et al., 2000). In previous studies, one of the most active metals for photocatalytic enhancement is platinum (Pt), which can produce the highest Schottky barrier among the metals that facilitate electron capture (Vorontsov et al., 1999). The capture of electrons by Pt is postulated to produce a longer electron-hole pair separation lifetime, and therefore hinder the recombination of electron/hole pairs and enhance the transfer of holes and possibly electrons to O₂ adsorbed on the TiO₂ surface. Afterwards, excited electrons migrate to the metal, where they become trapped and the electron/hole pair recombination is suppressed. Therefore, many investigations have reported the enhancement of photoactivities in both liquid

and gas phases results from depositing Pt (Hoffmann et al., 1995), although some recorded reverse effects.

Since TiO₂ has a wide-energy band gap, it limits the photosensitization to the visible light. To improve its response to visible light, various studies reported that TiO₂ doped with transition metal ions such as V, Cr, Mn, Fe, Ni or Au extends light absorption into the visible region (Serpone and Pelizzetti, 1989; Sun et al., 1998; Li and Li, 2001). Zang et al. (2000) reported an amorphous microporous titania modified with Pt, Rh, Au, Pd, Ni or Ir was capable of catalyzing the photodegradation of 4-chlorophenol in aqueous solution upon illumination with visible light. The band gap of titanium dioxide would be decreased and visible light absorption would be increased owing to the incorporation of Pt into the lattice of sol-gel titanium dioxide phase. But little literature related to the effect of Pt depositing on the surface of TiO₂ by means of photoreduction on optical absorption capability. However, the photoactivity enhancement of Pt-modified TiO₂ cannot simply be attributed to the capture of electrons by Pt and the Schottky barrier in the Pt facilitating the electron capture. Some research focused on the interaction of Pt with TiO₂ surface, and the effect of Pt on chemical state of Ti, energy level, and interfacial charge transfer (Serpone and Pelizzetti, 1989; Yang et al., 1997). This study characterizes the optical properties and the valence state of the catalyst Pt-TiO₂, charge carrier separation and photoactivity in the photodegradation of methylene blue (MB) and methyl orange (MO) as model reaction, in order to disclose the mechanism of photoactivity enhancement and photosensitization under visible light irradiation.

2. Experimental Methods

2.1 Preparation of Pt-TiO₂ Photocatalysts

TiO₂ powder was first prepared by a sol-gel process, in which sol was prepared by mixing titanium tetraisopropoxide, ethanol, water, and acetic acid at room temperature. Solution “A” was prepared by adding 17 ml Ti(O-Bu)₄ to 40 ml absolute ethanol. Next, solution “B” was prepared by mixing 60 ml absolute ethanol, 15 ml acetic acid, and 5 ml deionized distilled water. Then, solution “A” was added dropwise into solution “B” with vigorous stirring for 2 hrs. After the sol of TiO₂ formed and aged, the gel of TiO₂ was formed. TiO₂ powder was obtained after drying, grinding, and sintering at 923 K for 2 hrs (Sanchez and Lopez, 1995). The Pt-TiO₂ samples were then prepared by the photoreduction process (Yang et al., 1997; Yonezawa et al., 1999), according to the following procedure. The weighted amount of TiO₂ was suspended in a mixture of platinizing solution containing the required concentration of hexachloroplatinic acid in 0.1 M methanol solution, as a hole scavenger. The suspensions were irradiated with a 125 W mercury lamp. The irradiation lasted for 60 min. The molar content of Pt on TiO₂ was determined on the basis of the reduction of the Pt concentration in the mixture solution, which was detected by ICP (PS-1000AT). The Pt-TiO₂ samples were separated by filtration, washed repeatedly with deionized distilled water, and dried at 373 K for 24 hrs. The product samples had the Pt contents of 0.48%, 0.75%, 1.3%, and 2.6%.

2.2 Characterization of photocatalysts

The particle size of the catalysts was determined by a transmission electron microscopy (TEM). To determine the light absorption band edge, the UV-visible absorption spectra of the

photocatalysts were obtained in the range of 250 - 700 nm using a UV-visible Scanning Spectrophotometer (Shimadzu UV-2101 PC).

To study the recombination of electrons/holes, the photoluminescence (PL) of the samples was measured at room temperature by the following procedure. A 325 nm He-Cd laser was used as the excitation light source. The light from the sample was focused into a spectrometer (Spex500) and detected by a photo multiplier tube (PMT). The signal from the PMT was input into a photon counter (SR400) before being recorded by a computer.

To monitor the chemical state of photocatalysts, X-ray photoelectron spectroscopy (XPS) was recorded with a PHI Quantum ESCA Microprobe System, using the MgK_{α} line of a 250 W Mg X-ray tube as a radiation source with the energy of 1253 eV, 16 mA \times 12.5 kV. The working pressure was less than 1×10^{-8} Pa. As an internal reference for the absolute binding energies, the C 1s peak (at 284 eV) of hydrocarbon contamination was used. The fitting XPS curves were analyzed by Multipak 6.0A software.

2.3 Photocatalytic activity experiments

A cylindrical Pyrex photoreactor was used in this study, in which either a 110 W high-pressure mercury lamp with an emission of $\lambda > 365$ nm (Beijing Yaming Lamp Works) or a 110 W high-pressure sodium lamp with an emission of $\lambda > 420$ nm (Institute of Electrical Light Source, Beijing) was positioned inside the cylindrical Pyrex vessel surrounded by a circulating

water jacket (Pyrex) to cool the reaction solution. The photoemission spectra of both lamps are illustrated in Fig. 1.

[Fig. 1]

Analytical grade MB and MO were used as model dye chemicals. Their aqueous suspensions were prepared by adding 0.2 g photocatalyst powder to 165 ml of aqueous dye solution. Prior to irradiation, the suspensions were magnetically stirred in the dark for 15 min to establish the adsorption/desorption equilibrium of the dye. The aqueous suspensions containing dye were irradiated with constant aerating. At given irradiation time intervals, samples were taken from the suspension and immediately centrifuged at 70 rps for 20 min, then passed through a 0.45 μm Millipore filter to remove the particles.

2.4 Analytical methods

The concentrations of MB and MO were analyzed by Spectronic UV-visible spectroscopy (Genesys-2) at their maximum peaks in the visible region to evaluate the decolorization rate of MB and MO and the photoactivity of catalysts. Total organic carbon (TOC) concentration was monitored with a TOC analyzer (Shimadzu 5000A) equipped with an autosampler (ASI-5000). The concentrations of ammonium nitrogen, nitrite nitrogen, nitrate nitrogen, and sulfate ion formed during the reaction were determined by Ion Chromatography with conductivity detection (Shimadzu HIC-6A), in which a Shim-Pack IC-A1 anion column was used, and a mobile phase of 2.5 mM phthalic acid/2.4 mM tris(hydroxymethyl) aminomethane was used at a flow rate of 1.5

ml min⁻¹. A Shim-Pack IC-C1 cationic column was also used for the determination of ammonium ion, and a mobile phase of 5.0 mM nitrate acid was used at a flow rate of 1.0 ml min⁻¹.

3. Results and Discussion

3.1 Characteristics of Pt-TiO₂ catalyst

The primary particles of TiO₂ were first formed and analyzed by TEM. The TEM results revealed that the primary particles were highly crystalline, with a typical size of 20 - 30 nm. The specific surface area of the TiO₂ powder was 73 m² g⁻¹, as determined by ALTA AMI-100 instruments by N₂ adsorption at 77 K. The final particles of Pt-TiO₂ were analyzed by TEM and X-ray diffraction (XRD) methods. The results indicated that they had larger particle sizes of 40 - 80 nm and consisted of an anatase phase (85%) and a rutile phase.

3.1 Photocatalytic activity

To evaluate the photocatalytic activity of Pt-TiO₂ and determine the optimum content of Pt impurity, two sets of MB and MO suspensions were irradiated using the mercury lamp. The pseudo-first-order kinetics of the photodegradations are illustrated in Figs. 3A and B. The observed kinetic constants were calculated, and are listed in Table 1.

[Table 1]

The results in Table 1 indicate that the first-order kinetic constant increased with the increase of Pt content when it was below 0.75%, and decreased with the increase of Pt content when it was higher than 0.75%. This suggests that an optimum content of Pt impurity was 0.75% and any higher content of Pt impurity was detrimental to the enhancement of photoactivity. Choi et al. (1994) proposed that there appeared to be an optimal dopant concentration, above which the observed photoreactivity decreased. On the basis of the relevant band positions of Pt and TiO₂, Pt clusters at a lower concentration act as a separation center. The photogenerated electrons are transferred from TiO₂ conduction band to the Pt conduction band and the holes accumulate in the TiO₂ valence band. Hence, photogenerated electrons and holes were efficiently separated. However Pt clusters at a higher concentration act as a recombination center and the recombination rate between electrons and holes increases exponentially with the increase of Pt concentration because the average distance between trap sites decreases by increasing the number of Pt clusters confined within a particle.

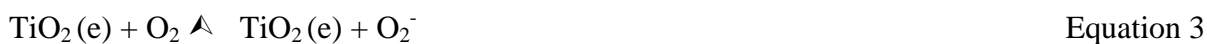
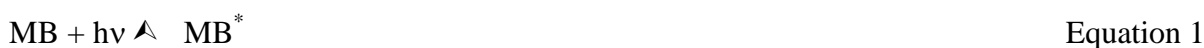
[Fig. 2]

The sodium lamp with visible light emission was also used as a radiation source to investigate the performance of the Pt-TiO₂ catalyst. The pseudo-first-order kinetics of MB and MO ($C_0 = 10 \text{ mg l}^{-1}$) photodegradations using the higher-pressure sodium lamp are illustrated in Figs 4A and 4B respectively. The observed kinetic constants of pure TiO₂ and 0.75% Pt-TiO₂ were 0.012 min^{-1} ($R^2 = 0.989$) and 0.0199 min^{-1} ($R^2 = 0.984$) respectively for the MB

photodegradation, and 0.0038 min^{-1} ($R^2 = 0.9866$) and 0.0162 min^{-1} ($R^2 = 0.9486$) respectively for the MO photodegradation.

[Fig. 3]

The first-order kinetic constant of 0.75% Pt-TiO₂ for the MO photodegradation was about 1.5 times that of pure TiO₂ when the mercury lamp was used as the radiation source, but 5 times that of pure TiO₂ when the sodium lamp was used. However, the first-order kinetic constant of 0.75% Pt-TiO₂ for the MB photodegradation indicated that the both reaction rates using the two lamps were 1.5 times that of the pure TiO₂. This might be the reason why MB is a dye sensitizer and can be excited by visible light, as described in Equations 1 - 3 below. Under the visible light irradiation from the sodium lamp, MB could be excited directly, and the excited MB molecules injected electrons into the conduction band of TiO₂, after which the electrons were scavenged by oxygen adsorbed on the surface of TiO₂. In the other case, MO could not be excited by the sodium lamp emission, and was slowly photodegraded with pure TiO₂.



TOC in the reactions was monitored to investigate the mineralization of MB and MO. The experimental results are shown in Fig. 4. The experiment demonstrated that the TOC

concentration of MB and MO solutions significantly decreased after irradiation using either the mercury lamp or the sodium lamp. The TOC removals using the pure TiO_2 and 0.75% Pt- TiO_2 in the MB photodegradation under the irradiation of the mercury lamp for 60 min were 63% and 82%, and in the MO photodegradation were 64% and 85%. The TOC removals using the pure TiO_2 and 0.75% Pt- TiO_2 in the MB photodegradation were 40% and 72%, and in the MO photodegradation were 27% and 70% under the irradiation of sodium lamp for either 60 min or 150 min.

[Fig. 4]

To evaluate the products formed in the MB and MO photodegradation, samples were collected at 0, 12, 24, 36, 48, and 60 min during the reaction, and measured by ion chromatography for determination of ammonia nitrogen, nitrite nitrogen, nitrate nitrogen and sulfate ions. The results are illustrated in Figs 5 and 6. It can be seen that sulfate and nitrate ions were the main products from the MB and MO photodegradation. In this experiment, the photocatalytic reaction conducted a nitrogen conversion from organic forms into inorganic forms. During the reactions, ammonium ion may be an intermediate product and further oxidized into nitrite and nitrate ions. The mass balances between organic and inorganic nitrogen in different reactions are compared in Table 2. The results demonstrated that the nitrogen conversion rate using the modified TiO_2 catalyst were significantly higher than the conventional TiO_2 . The results also indicated that the nitrogen conversion in MB photodegradation achieved a higher portion than that in MO photodegradation.

[Fig. 5]

[Fig. 6]

[Table 2]

3.2 Chemical and electronic structure of Pt-TiO₂

XPS analyses were carried out to determine the chemical and electronic structure of powders and the valence states of various species present therein. The Ti 2p, O 1s, and Pt 4f XPS spectra of samples are shown in Figs 7A - C. The intensity and positions of PL peaks were calculated by Multipak 6.0A software, and are listed in Table 3.

[Table 3]

The XPS spectra of the pure TiO₂ and 0.75% Pt/TiO₂ are shown in Fig. 7. In Fig. 7A, the Ti 2p XPS peaks of the pure TiO₂ with slight asymmetry are narrow and have a binding energy of 459 eV (FWHM = 1.14 eV) attributed to Ti⁴⁺. The XPS spectra of the 0.75% Pt-TiO₂ showed the presence of two peaks matching the trivalent and tetravalent states of Ti. It is clear that the presence of Ti³⁺ arose from the depositing of Pt on the surface of TiO₂. In some instances (Vogt et al., 1994; Xiao et al., 1998; Rahman et al., 1999), both Ti²⁺ and Ti³⁺ states along with Ti⁴⁺ can be present, owing to Pb-, Nd-doped, or Ar ion bombardment. In our investigation, the formation of Ti³⁺ implies that the interaction between Pt and the TiO₂ matrix occurred during photoreduction. However, the O 1s XPS spectra show a wide peak structure for 0.75% Pt-TiO₂,

as illustrated in Fig. 7B and Table 4. The peak at 529 eV (FWHM = 1.36 eV) for 0.75% Pt-TiO₂ was in agreement with O 1s electron binding energy for TiO₂ molecules. For the pure TiO₂, the O 1s peak with slight asymmetry was narrow and had a binding energy of 529 eV (FWHM = 1.27 eV). In Fig. 7C, the Pt 4f peak of 0.75% Pt-TiO₂ consisted of four individual peaks, corresponding to metallic Pt, Pt(OH)₂, PtO₂, and PtCl₆²⁻ respectively. The peak at 71.3 eV can be attributed to metallic Pt, the peak at 73.1 eV was peculiar to Pt(OH)₂, the peak at 74.8 eV was due to PtO₂, and the peak at 77.2 eV to PtCl₆²⁻ from the handbook of Multipak 6.0A software. Pt-TiO₂ was prepared by the photoreduction. At first, PtCl₆⁻ was adsorbed on the surface of TiO₂, then reduced into PtCl₄⁻ and Pt⁰ or (Pt⁰)_m. However, PtCl₆⁻ was only partially photoreduced. The change of Pt valence state versus photoreduction time was monitored by XPS. Moreover, Vorontsov et al. (1999) reported that different pH values and different acetic acid concentrations during the photocatalytic deposition could result in different Pt deposit forms and the Pt binding energy of Pt metal, Pt(OH)₂, PtO₂, and PtCl₆²⁻ was 70.5 eV, 72.4 - 73.2 eV, 74.1 - 75.5 eV, 77.5 eV respectively. Yang et al. (1997) reported the similar results. The different species of Pt on the surface of TiO₂ have different photoactivity and optical absorption properties. Therefore, the photosensitization of Pt-TiO₂ samples to visible light was partially caused by the presence of Pt, Pt(OH)₂, and PtO₂ on the surface of TiO₂.

[Fig. 7]

[Table 4]

3.3 Mechanism of visible light photosensitization

The UV-visible absorption spectra were measured to express the optical absorption properties of photocatalysts, as shown in Fig. 8. The optical absorption enhanced significantly in the region of 300 - 700 nm, owing to the presence of Pt, in comparison to the pure TiO₂. Although it is clear that the optical absorption edges significantly shifted to the red direction, there was no significant optical absorption peak in the visible region.

[Fig. 8]

The mechanism of visible light photosensitization can be explained in the following two ways. Firstly, the metallic Pt, Pt(OH)₂, and PtO₂ deposited on the surface of TiO₂ can significantly absorb visible light. The enhancement of visible optical absorption due to the presence of Pt, Pt(OH)₂ and PtO₂ has been proven by UV-visible reflectance spectra (Alexander et al., 1999). Secondly, some energy levels can be produced in the band gap of TiO₂ by the dispersion of Pt nanoparticles in the TiO₂ matrix. The surface state between Pt nanoparticles and the TiO₂ matrix might play an important role in producing lower energy levels within the TiO₂ band gap. Some papers have confirmed the existence of defect energy levels attributable to Ti³⁺, the position of which is near the TiO₂ valence band (Mizushima et al., 1979). As shown in Fig. 9, when $E_g > h\nu > (E_c - E_f)$, electrons can be excited from the defect state to the TiO₂ conduction band. Perhaps the defect energy level was one of the reasons why 0.75% Pt-TiO₂ could maintain high photoactivity in photodegraded MO irradiated by the sodium lamp.

[Fig. 9]

3.4 PL emission spectra and the recombination of electron/hole

The PL emission spectra are useful to disclose the efficiency of charge carrier trapping, immigration, and transfer, and to understand the fate of electron-hole pairs in semiconductor particles since PL emission results from the recombination of free carriers. In this study, the PL emission spectra of all samples were examined in the range of 3 - 3.8 eV and 1.8 - 3 eV and are shown in Fig. 10. To illustrate the results, the positions of individual PL emission peaks are listed in Table 2. The PL emission spectra of the pure TiO₂ sample, as shown in Fig. 10A, revealed that several peaks appeared at 3.32 eV, 3.27 eV, 3.21 eV, and 3.12 eV, which were equivalent to the 373.5 nm, 379.5 nm, 385.5 nm and 397 nm wavelengths. The PL emission spectra of the 0.75% Pt-TiO₂ and pure TiO₂ showed similar positions for most peaks, but with different PL intensities. The PL intensity of the pure TiO₂ sample was significantly higher than that of the 0.75% Pt-TiO₂. If it is agreed that the PL emission mainly results from the recombination of excited electrons and holes, then a lower PL intensity might indicate a lower recombination rate of those electrons and holes under light irradiation. As all of the samples exhibited a mixture of anatase and rutile phases, the main peaks at 3.32 eV (or 3.31 eV) and 3.27 eV (or 3.26 eV) are the band gaps of the anatase phase, and the peaks at 3.22 eV (or 3.21 eV) and 3.12 eV (or 3.11 eV) are the band gaps of rutile phase – which are very similar to the results reported by Tang et al. (1994) and Suisalu et al. (1998). Some other small peaks also appeared in the PL emission spectra, and they were attributable to quantum size. Comparing our experimental results to those of other researchers, it can be concluded that the Pt deposited on TiO₂ does not change the band edge of anatase and rutile very much, but can reduce PL emission significantly. The PL emission spectra of all

samples in the 1.8 - 3 eV (420 – 700 nm) range are shown in Fig. 10. An intensive yellowish green PL spectrum (broad band) of the pure TiO₂ was much higher than any other spectra of the 0.75% Pt-TiO₂ samples. These results indicate that the position of the PL peaks apparently shifted to the red direction due to the presence of Pt impurity.

The less recombination of electrons/holes in the Pt-TiO₂ catalyst can be explained in the following manner. Firstly, the excited electrons from the valence band to the conduction band migrated to Pt clusters, then migrated to O₂ molecules adsorbed on the surface of the Pt. The Pt deposited on the TiO₂ surface produced the highest Schottky barrier among the metals that facilitated the electron capture. Secondly, Pt⁴⁺ species trapped the excited electrons, which migrated to O₂. The overall process of charge carrier trapping, migration, and transfer was promoted due to the presence of Pt. Thirdly, the defect energy level might act as a separation center. Ti³⁺ could enhance the oxygen chemisorption and promote the excited electrons trapped by O₂. Therefore, the enhancement of photoactivity has a good agreement with the decrease of PL intensity.

[Fig. 10]

4. Conclusions

The photocatalytic oxidation of MB and MO in aqueous solutions was promoted with the existence of Pt impurity deposited on the TiO₂ surface. The optimal content of Pt was found to be

0.75%. Specifically, the observed first-order kinetic constant of MO photodegradation using the 0.75% Pt-TiO₂ was 5 times that of using the pure TiO₂.

The experimental results confirmed the existence of Pt⁰, Pt²⁺, and Pt⁴⁺ species on the surface of the Pt-TiO₂ and Ti³⁺ in its lattice. The interaction of Pt impurity and the crystal surface of TiO₂ might be a reason to improve its photocatalytic properties.

The experimental results demonstrated that the TiO₂ doped with Pt has a stronger absorption of visible light and a lower intensity of PL emission than conventional TiO₂.

Acknowledgement

The authors wish to thank the Hong Kong Government Research Grant Committee for a financial support to this work under the RGC Grant (RGC No: PolyU 5030/98E).

References

Alexander, V., Evgueni, N., Savinov, Jin Z.S., 1999. Influence of the form of photodeposited Pt on titania upon its photocatalytic activity in CO and acetone oxidation. *J. Photoch. Photobio. A* 125,113-117.

Choi, W.Y., Termin, A., Hoffmann, M.R., 1994. The role of metal ion dopants in quantum-sized TiO₂: Correlation between photoreactivity and charge carrier recombination dynamics. *J. Phy. Chem.* 98(51), 13669-13679.

- Goswami, D.Y., 1997. A review of engineering developments of aqueous phase solar photocatalytic detoxification and disinfection processes. *J. Sol. Energ-T ASME*. 119(5), 101-106.
- Hoffmann, M.R., Martin, S.T., Choi, W.Y., Bahnemann, D. W., 1995. Environmental Applications of Semiconductor Photocatalysis. *Chem. Rev.* 95, 69-96.
- Li, X.Z., Li, F.B., 2001. Study of Au/Au³⁺-TiO₂ Photo-catalysts Toward Visible Photo-Oxidation For Water and Wastewater Treatment. *Environ. Sci. Technol.* 35, 2381-2387.
- Linsebigler, A., Lu, G., Yates, J.T., 1995. Photocatalysis on the TiO₂ surfaces: principles, mechanisms, and selected results. *Chem. Rev.* 95, 735-758.
- Mizushima, K., Tanaka, M., Asai, A., S. Iida, S., 1979. Impurity levels of Iron-group ions in TiO₂ (II). *J. Phys. Chem. Solids*. 40, 1129-1140.
- Rahman, M.M., Krishna, K.M., Soga, T., Jimbo, T., Umeno, M., 1999. Optical properties and X-ray photoelectron spectroscopic study of pure and Pb-doped TiO₂ thin films. *J. Phys. Chem. Solids*. 60, 201-210.
- Sanchez, E., Lopez, T. 1995. Effect of the preparation method on the band gap of titania and Pt-titania sol-gel materials. *Materials Letters*. 25, 271-275.
- Serpone, N., Pelizzetti, E. 1989. Edited, *Photocatalysis Fundamentals and Application*. Edit II, Wiley-Interscience, New York, 236.
- Suialu, A., Aarik, J., Mändar, H., Sildos, I., 1998. Spectroscopic study of nanocrystalline TiO₂ thin films grown by atomic layer deposition. *Thin Solid Films* 336, 295-298.
- Tang, H., Berger, H., Schmid, P., Levy, F., 1994. Optical properties of anatase (TiO₂). *Solid State Commun.* 92, 267-271.

- Vogt, K.W., Kohl, P.A., Carter, W.B., Bell, R. A., Bottomley, L. A., 1994. Characterization of thin titanium oxide adhesion layers on gold: resistivity, morphology, and composition. *Surf. Sci.*, 301, 203-213.
- Vorontsov, A.V., Savinov, E.N., Jin, Z.S., 1999. Influence of the form of photodeposited Pt on titania upon its photocatalytic activity in CO and acetone oxidation. *J. Photoch. Photobio. A* 125, 113-117.
- Vorontsov, A.V., Stoyanova, I.V., Kozlov, D.V., Simagina V. I., Savinov E.N., 2000. Kinetics of the photocatalytic oxidation of gaseous acetone over platinized titanium dioxide. *J. Catal.*, 189, 360-369.
- Xiao, Z.D., Su, L.Y., Gu, N., Lu, Z.H., Wei, Y., 1998. The growth of TiO₂ thin films on mixed self-assembly monolayers from solution. *Thin Solid Films*. 333, 25-28.
- Yang, J.C., Kim, Y.C., Shul, Y.G., Shin, C.H., Lee, T.K., 1997. Characterization of photoreduced Pt/TiO₂ and decomposition of dichloroacetic acid over photoreduced Pt/TiO₂ catalysts. *Appl. Surf. Sci.* 121/122, 525-529.
- Yonezawa, T.; Matsune, H.; Kunitake, T. 1999. Layered nanocomposite of close-packed gold nanoparticles and TiO₂ gel layers. *Chem. Mater.* 11, 33-35.
- Zang, L., Macyk, W., Lange, C., Maier, W.F., Antonius, C., Meissner, D., Kisch, H. 2000. Visible-light detoxification and charge generation by transition metal chloride modified titania. *Chem-Eur. J.* 6(2), 379-384.